J. Basic. Appl. Sci. Res., 3(7)75-83, 2013

ISSN 2090-4304
Journal of Basic and Applied Scientific Research
www.textroad.com

Improvement Fault Ride through Capability of Fixed-Speed Turbines by Unified Power Flow Controller (UPFC)

Yaser Mohammadi, Mehdi Radmehr

Department of Electrical Engineering, Azad University Sari Branch, Sari, Iran

ABSTRACT

Fault ride-through (FRT) is required for wind turbines connected to the grid, which is steadily increasing in recent years. This paper presents a solution for wind energy conversion system based on use unified power flow controller (UPFC) for improving FRT. The wind energy conversion system (WECS) is considered as a fixed-speed system, equipped with a squirrel-cage induction generator. The drive-train is represented by two-mass model. The analytical and simulation studies of the UPFC and proposed control scheme for improving FRT capability are presented and compared with the impact of the application of the STATCOM. The simulation results show that UPFC can improve the FRT capability of WECS compare to STATCOM. PSCAD/EMTDC software is used for simulation.

KEYWORDS: Unified Power Flow Controller (UPFC), Static Synchronous Compensator (STATCOM), Wind Energy conversion system (WECS), Fixed Speed Wind Turbine (FSWT), Induction Generator (IG).

I. INTRODUCTION

As a clean and renewable energy, the wind energy resources have dramatically increased over the past decade. Fault ride-through (FRT) is now required for connection of wind farms in most power systems. The FRT-compliant wind farm must remain connected and actively contribute to system stability during a wide range of network fault scenarios. FRT is particularly important in securing stability in regions where wind is becoming a significant contributor to the power system's dynamic performance. The wind industry has responded to the introduction of FRT requirements in several ways according to wind turbine technology type [1-3].

There are two main types of wind turbines: the fixed speed wind turbine (FSWT) and the variable speed wind turbine (VSWT). There is a growing trend towards variable speed turbines by manufacturers because variable VSWT have higher efficiency and greater flexibility. Nevertheless, over the last years, FSWT have been installed in large proportions in power grids. As wind parks have a lifetime of over 20 years, it is still a matter of interest to investigate the interaction of FSWT with power systems [4-5].

However, a wind farm implemented using FSIG based wind turbine has difficulties in meeting the proposed Grid Code in terms of the fault ride through, reactive power and voltage control requirements. Previous research has revealed that faults which occur on the transmission line can lead to wind generator over-speed and cause instability of the network Voltage [5-6].

When, fault occurs, the terminal voltage of IG drops. Therefore, the electrical torque abruptly deceases to zero due to the terminal IG voltage and the rotor speed starts to increase. After fault clearance, the reactive power consumption increases resulting in reduced voltage of IG. Thus the induction generator voltage does not recover immediately after fault, but a transient period follows. Therefore, the generator continues to accelerate and the generator becomes unstable [4-6].Thus, by providing the needed reactive power not only improves voltage regulation, but also helps to damp the rotor speed oscillations.

In this paper, UPFC is used for solving FRT problems of the interaction of wind energy conversion system (WECS) and power grid. Many papers have been discussed the using of shunt FACTS controllers like SVC and STATCOM to improve the Fault ride-through of WECS [6-8]. But, they aren't impact during fault and do not provide damping of speed oscillations. UPFC consists of a series and a shunt converter connected by a common DC link capacitor. The series converter of UPFC, by injecting a series voltage in quadrature with the line current acts as large inductor to prevent dip voltage drop during fault. On the other hand, the shunt converter of the UPFC aims to restore the voltage at the terminals of the generator and thereby mitigate the destabilizing electrical torque and power after fault clearing.

The scientific contributions of this paper are:

1) The series converter of UPFC, suppresses the instantaneous voltage drop and it is able to improve transient behavior of WECS during fault, which is the main advantage of the UPFC to STATCOM and SVC.
2) The shunt converter of the UPFC by injecting reactive power aims to restore the voltage at the terminals of the generator and improve the generator transient stability after fault clearing after fault clearing.

The simulation results show that FRT capability of WECS is improved by using UPFC. Also, the simulation results show that UPFC can improve the FRT capability of WECS compare to STATCOM.

*Corresponding Author: Yaser Mohammadi, Department of Electrical Engineering, Azad University Sari Branch, Sari, Iran

II. UNIFIED POWER FLOW CONTROLLER (UPFC)

The configuration of a typical UPFC is shown in Fig. 1. It consists of a series and a shunt converter connected by a common DC link capacitor. Series and shunt converters connected in series and shunt by boosting transformer (B_T) and Exciting transformer (E_T) respectively. The shunt converter of UPFC controls the UPFC bus voltage/shunt reactive power and DC capacitor voltage. The series converter of UPFC controls the transmission line active and reactive power flow by injecting a series voltage of adjustable magnitude and phase angle. The interaction between the series injected voltage and the transmission line current leads to active and reactive power exchange between the series converter and power system [9].

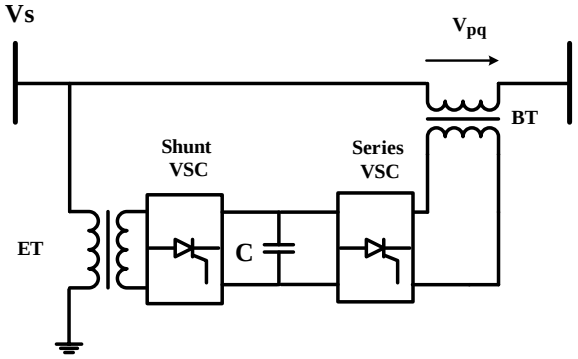

Fig. 1: UPFC schematic diagram

The series converter of UPFC controls the line active and reactive power flow by injecting a series voltage of adjustable magnitude and phase angle.

Under steady state condition, series converter provides the main function of UPFC by injecting a voltage V_{pq} with controlled magnitude ($0<V_{pq}<V_{pqmax}$) and angle ρ, ($0<\rho<2\pi$) in series with the transmission line, and controls power flow of the line. The phasor diagram of this mode is shown in Fig.2, where V_S represents sending end voltage, V_r receiving end voltage, V_{pq} is UPFC voltage, which is inserted to the power system through the series transformer, X_L is transmission line reactance and I is the line current.

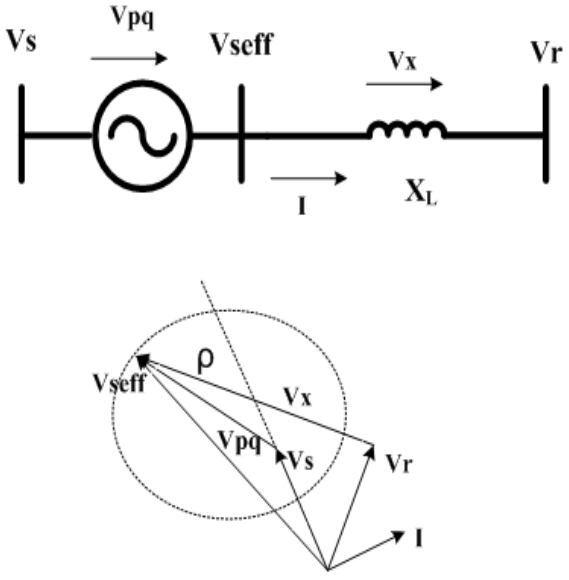

Fig. 2: Phasor diagram of UPFC in normal condition

III. MODELING OF WECS

Fig. 3 shows the schematic diagram of a typical WECS. The wind speed model, the model of wind turbine, the mechanical model of the drive-train and induction generator is described in the following sections.

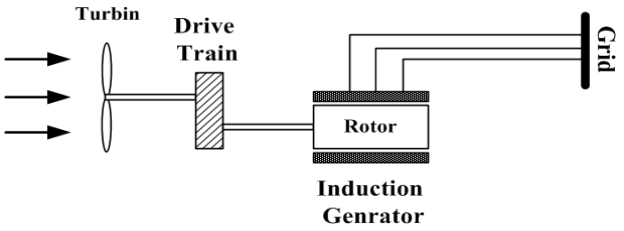

Fig. 3: Schematic diagram of typical WECS

A. WIND SPEED MODEL

As shown in Fig. 4, wind speed is modeled as the sum of following component:
Base wind speed $v_{wa}(t)$,
Gust wind speed $v_{wg}(t)$,
Ramp wind speed $v_{wr}(t)$ and
Noise wind speed $v_{wt}(t)$ [10].
The Steady wind speed to the turbine [m/s] is 15 m/s.

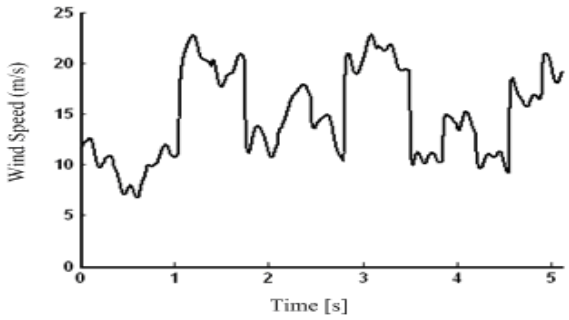

Fig. 4: Wind Speed Model

B. WIND TURBINE MODEL

In general, the relation between wind speed and mechanical power extracted from the wind can be described, as follow [10]-[11]:

$$P_{wt} = \frac{\rho}{2} A_{wt} C_p(\lambda, \beta) \vartheta_w^3 \quad (1)$$

where, P_{wt} is the power extracted from the wind, ρ is the air density, v_w is the wind speed, CP is the performance coefficient or power coefficient, λ is the tip speed ration, A_{wt} is the area covered by the wind turbine rotor. Fig. 5 shows the C_p - λ curve. The performance coefficient is different for each turbine and is relative to the tip speed ratio λ and pitch angle β. In this paper, the C_p is, as follows [12]:

$$C_P = \frac{1}{2}(\lambda - .022\beta^2 - 5.6)e^{-0.17\lambda} \quad (2)$$

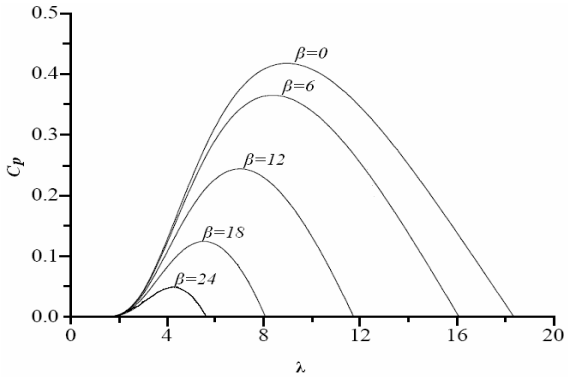

Fig. 5: C_P- λ curves for different pitch angles

C. SHAFT MODEL / DRIVE TRAIN SYSTEM

The shaft model of the wind turbine is described by the two-mass model as shown in Fig. 6 and defined by the following equation [11]:

$$\frac{\partial \theta_s}{\partial t} = \omega_t - \omega_g \tag{3}$$

$$\frac{\partial \omega_t}{\partial t} = \frac{1}{2H_t}(T_t - K_s\theta_s + D(\omega_g - \omega_t)) \tag{4}$$

$$\frac{\partial \omega_g}{\partial t} = \frac{1}{2H_g}(-T_e + K_s\theta_s - D(\omega_g - \omega_t)) \tag{5}$$

Where,

$\boldsymbol{T_t}$ the mechanical torque referred to the generator side,
$\boldsymbol{T_e}$ the electromagnetic torque,
$\boldsymbol{H_t}$ the equivalent turbine-blade inertia,
$\boldsymbol{H_g}$ the generator inertia,
$\boldsymbol{\omega_t}$ the turbine's rotational speed,
$\boldsymbol{\omega_g}$ the generator's rotational speed,
$\boldsymbol{K}$ the shaft stiffness
$\boldsymbol{D}$ the damping constant
$\boldsymbol{\theta_s}$ the angular displacement between the ends of the shaft

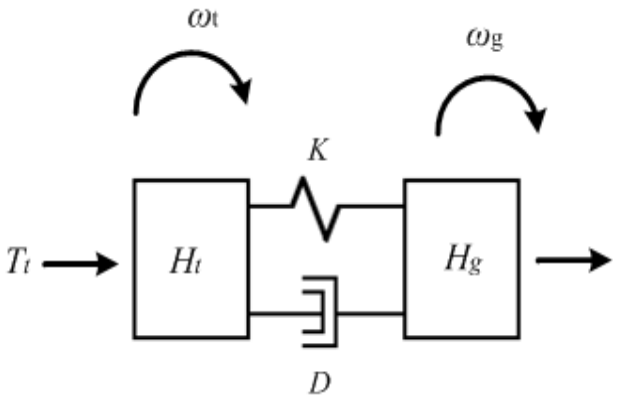

Fig. 6: Two mass model of wind turbine train

IV. EFFECT OF UPFC DURING FAULT

The concept of the induction generator stability can be further explained by using the electrical torque versus rotor speed curve of an induction generator. In order to obtain a mathematical relationship between electrical torque and rotor speed, the steady-state equivalent circuit of an induction generator shown in Fig. 7 is used [12].

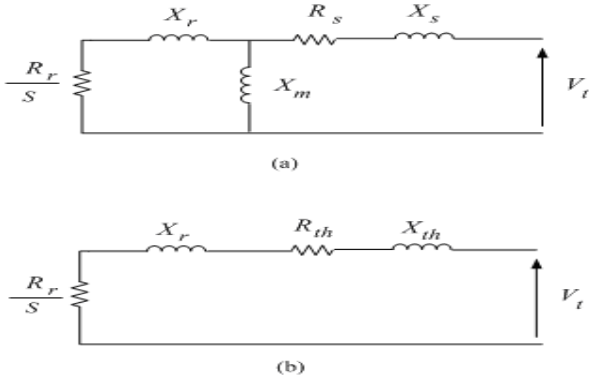

Fig. 7: Steady-state equivalent circuit of induction generator (a), complete model and (b) Thevenin model.

Where, R_r, R_s *and* R_{th} are the rotor, stator and the venin resistance, respectively. X_r, X_s, X_m *and* X_{th} is the rotor, stator, magnetizing and the venin reactance, respectively. Also V_t *and* V_{th} are the terminal and thevenin voltages, respectively and I_r *and* I_s the rotor and stator currents, respectively. In this equation, $s = (\omega_s - \omega_r)/\omega_s$ is the rotor slip and ω_s *and* ω_r are the synchronous and rotor speeds, respectively.

The electrical torque, T_e can be calculated, as follows:

$$T_e = \frac{R_r}{s} I_r^2 = \frac{R_r}{s} \frac{V_{th}^2}{(R_{th} + R_r / s)^2 + (X_{th} + X_r)^2} \quad (6)$$

When the induction machine operates as a generator, the mechanical torque is negative. Therefore, the electrical-mechanical equilibrium equation of an induction generator can be written, as follows:

$$\frac{d\omega_r}{dt} = \frac{(T_e - T_m)}{2H} \quad (7)$$

where, H is the inertia constant. From Eq (7), two equilibrium points, where the electrical torque is equal to the mechanical torque, can be found.

The power system shown in Fig. 8, has been used to study the effect of the UPFC on the performance of the induction generator after occurrence of a three-phase short circuit. Fig. 9 shows the equivalent circuit of the system with UPFC during fault. During fault condition, the large fault currents would flow through the UPFC during a downstream fault. This will cause the voltage at terminal of IG to drop, which would affect operation of shunt inverter of UPFC.

Furthermore, if not controlled properly, the UPFC might also contribute to this PCC voltage sag in the process of compensating the missing voltage, thus further worsening the fault situation. Therefore, the electrical torque abruptly deceases to zero due to the terminal IG voltage and the rotor speed starts to increase.

To restore the terminal voltage and the electrical torque of IG, UPFC act as a large virtual inductance in series with the line in fault situations. Controlling the UPFC as a virtual inductor would also ensure zero real power absorption and thus minimize the stress in the dc link during fault. On the other hand, the UPFC aims to increase the voltage at the terminals of the WECS and thereby mitigate the destabilizing electrical torque and power during the fault.

By representing the UPFC as an inductance, the reactance in series can be recalculated as:

$$X_{pq} = \frac{V_{pq}}{I} \quad (8)$$

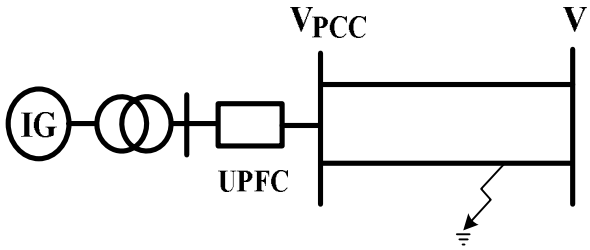

Fig. 8: Study power system

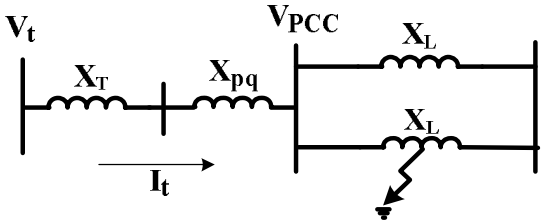

Fig. 9: Equivalent circuit of system with UPFC during fault

The terminal voltage of IG is determined by the following equation:

$$V_t = V_{PCC} - (X_T + X_{PCC}) I_t \quad (9)$$

Assuming V is constant during the fault, the terminal voltage of IG is determined by I_t. By using UPFC, I_t is limited and a voltage sag is prevented at PCC and terminal voltage of induction generator (Vt). Fig. 10 shows the electrical torque versus rotor speed curve with UPFC.

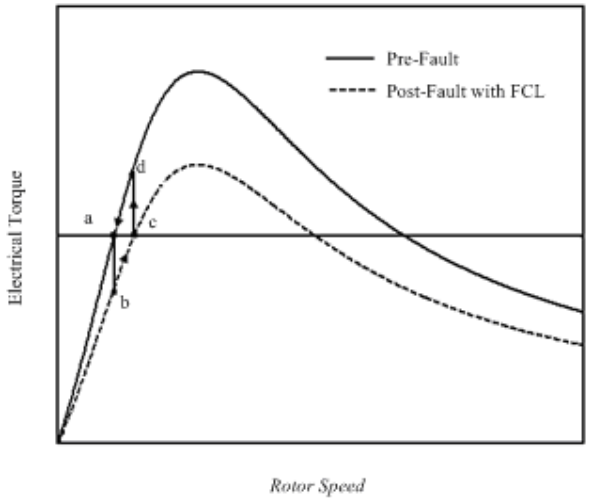

Fig. 10: Electrical torque versus rotor speed curve with UPFC during fault.

Before the fault occurrence, the generator is in operating point "a". At fault instant, the electrical torque is abruptly decreases and generator operating point moves to point "b". As a result, the rotor speed starts to increase according to post fault curve and reaches to equilibrium point "c" and be stable at this point, during the fault. At instant tc, the fault is eliminated and the generator operating point change to "c". At this instant, the rotor speed starts to decreases, since the net torque (Te-Tm) is negative and eventually the generator will return to operate at point "a". Therefore, the application of the UPFC in faulted feeder has two effects, as follows:

1- The voltage sag is prevented at the terminal voltage of induction generator (V_t) during fault. On the other hand, the shunt converter of the UPFC aims to restore the voltage at the terminals of the generator .According to Eq(6), the electrical torque is proportional to the square of the terminal voltage. Therefore, UPFC prevents from the decreasing electrical torque and accelerating the induction generator.

2- As shown in Fig. 10, UPFC prevents from increasing speed independent of fault clearing time. According Eq(6), the electrical torque is inversely proportional to slip and rotor speed. Therefore, UPFC prevents from decreasing electrical torque and accelerating induction generator.

V. SIMULATION RESULTS

- A single line diagram of the simulated power system with UPFC is shown in Fig. 11. The parameters of this system are listed in appendix A. A three phase short circuit fault is simulated on the middle of line, which starts at t=10s. After 0.2 s, the circuit breaker isolated the faulted line. The simulations have been carried out by PSCAD/EMTDC for Three cases, as follows:
- Case A: Without using any UPFC and STATCOM,
- Case B: By using STATCOM,
- Case C: By using UPFC.

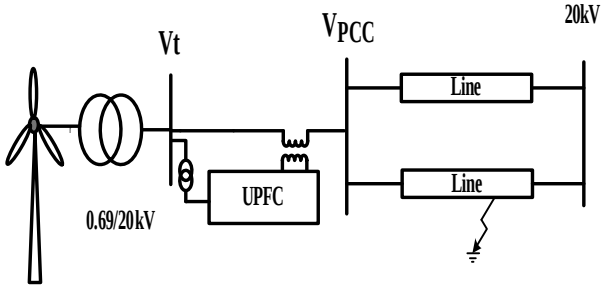

Fig. 11: Simulated power system with UPFC

Fig. 12 shows the rms value of the terminal voltage of IG for three cases. It can be observed that terminal voltage of IG decreases to zero in cases B and A, approximately during fault and in case A cannot be restored to pre-fault level. The UPFC

not only decreases the voltage sag to 0.6 pu, but also the voltage at PCC can be restored quickly after the fault compare to case B.

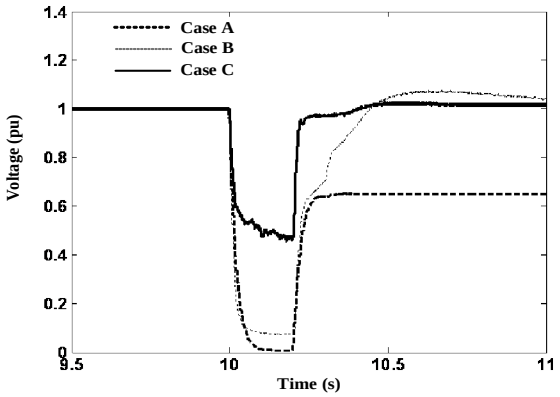

Fig. 12: Effect of UPFC on terminal voltage during fault

Fig. 13 and Fig. 14 show the active and reactive power exchanged between the IG and the grid for three cases, respectively. After the fault, the active power is restored by using the UPFC and STATCOM in cases B and C. As shown in Fig. 14, the absorbing reactive power from the grid is significantly reduced by using UPFC, which helps to avoid other problems such as voltage collapse.

Figures 15 and 17 show the electrical torque and the rotor speed of the induction generator for three cases, respectively. As shown in Fig. 15, the variation of the electrical torque is reduced in both cases B and C, and restored in pre-fault value. But, the UPFC is very effective in suppressing the variations of the electrical torque and swings after fault clearing. Fig 16 shows the enlargement of Fig. 15.

As shown in Fig.17, the rotor speed gradually reduces to the pre-fault level and the system is stable in both cases B and C, but the UPFC can provide a better damping to post-fault oscillations.

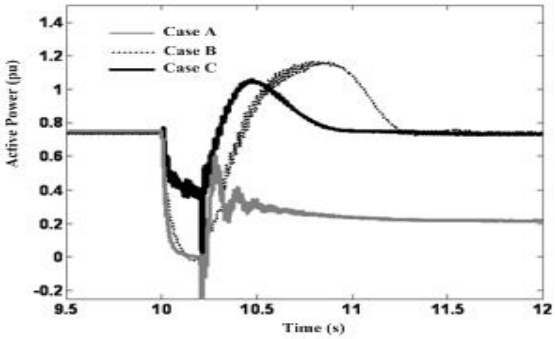

Fig. 13: Active power during fault

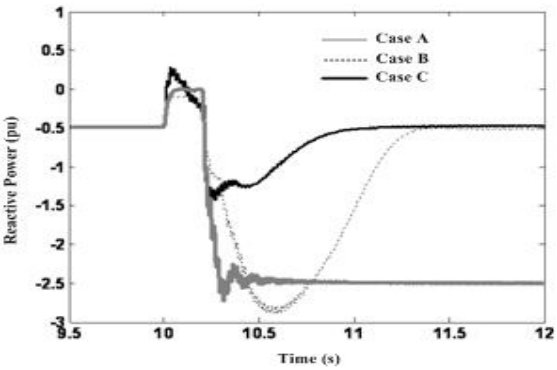

Fig. 14: Reactive power during fault

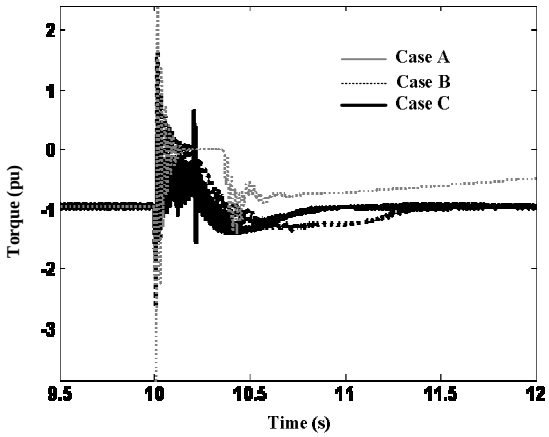

Fig. 15: Electrical torque of induction generator during fault

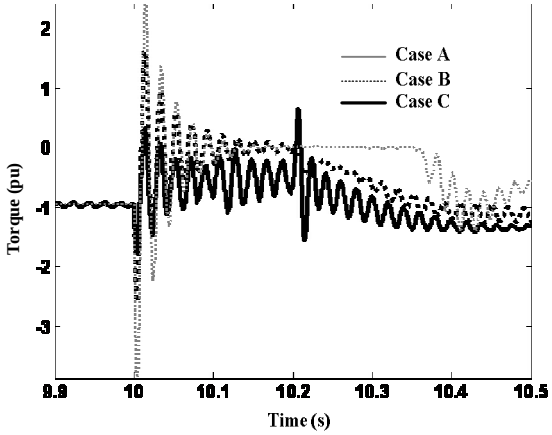

Fig. 16: Enlargement of Fig 14

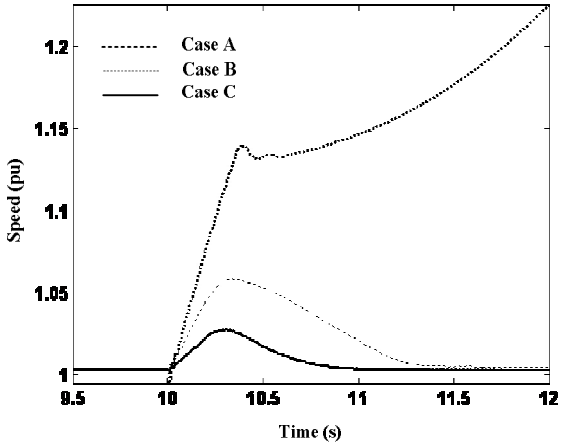

Fig. 17: Rotor speed of induction generator during fault

VI. CONCLUSION

In this paper, the effect of the UPFC in the performance of fixed speed turbines has been studied based simulation by PSCAD/EMTDC. The simulation results show that the UPFC not only suppresses the voltage drop but also improves generator speed and the voltage stability of power grid integrated with WECS. Also, the comparison with STATCOM shows that the UPFC is more effective for enhancement of FRT capability than STATCOM.

VII.APPANDIX A

GRID	
Supply	20 kV
Frequency	50Hz
Step down	.69kV/20 kV
transformer	,10 MVA
X/R ratio	8

INDUCTION GENERATOR	
Number of poles	4
Slip	1.8%
Power factor	0.9
Stator resistance	0.0577 Ω
Rotor resistance	0.0161 Ω
Stator reactance	0.0782 Ω
Rotor reactance	0.012 Ω
Magnetizing reactance	2.43 Ω

REFERENCES

[1] J. F. Manwell, J. G. McGowan, and A. L. Rogers, Wind energy explained, John Wiley, 2002.

[2] Thomas Ackermann , " Wind power in power systems " Copyright @ 2005 John Wiley & Sons, Ltd

[3] Tony Burton, David Sharpe, " Wind energy handbook " Copyright @ 2001 by John Wiley & Sons, Ltd

[4] Juan M. Rodriguez, Jose L. Fernandez, "Incidence on power system dynamics of high penetration of fixed speed and doubly fed wind energy systems: study of the Spanish case " IEEE Transactions on power system, Vol. 17, No. 4, November 2002

[5] H. S. Ko, G. G. Yoon, and W. P. Hong, "Active use DFIG-based variable- speed wind-turbine for voltage control in power system operation,"*J. Elect. Eng. Technol.*, Vol. 3, No. 2, pp. 254–262, Jun. 2008.

[6] M. Aten, J. Martinez, and P. J. Cartwright, "Fault recovery of a wind farm with fixed speed induction generators using a STATCOM," *Wind Eng*, Vol. 29, No. 4, PP. 365–375, 2005.

[7] S. M. Muyeen, M. A. Mannan, M. H. Ali, R. Takahashi, T. Murata, and J. Tamura, "Stabilization of wind turbine generator system by STATCOM," *IEEJ Trans. Power Energy*, Vol. 126, No. 10, Oct. 2006.

[8] H. Gaztanaga, I. E. Otadui, D. Ocnasu, and S. Bacha, "Real-time analysis of the transient response improvement of fixed-speed wind farms by using a reduced-scale STATCOM prototype," *IEEE Trans. Power Syst.*, Vol. 22, No. 2, PP. 658–666, May 2007.

[9] Narain G.Hingorani, "High Power Electronics and Flexible AC Transmission System," IEEE. Power Engineering Review, pp. 3-4, julay 1998

[10] Control Design And Performance Analysis Of A 6 Mw Wind Turbine Generator, IEEE Transactions On Power Apparatus and Systems, Vol. PAS 102, No. 5, May 1983, pp. 1340-1347.

[11] P. M. Anderson and Anjan Bose, "Stability Simulation of Wind Turbine Systems," IEEE Transactions on Power Apparatus and Systems, Vol. PAS-102, No.12, pp.3791-3795, Dec 1983

[12] B. Adkins and R. G. Harley, The General Theory of Alternating Current Machines, London, UK: Chapman & Hall, 1975.